

# Dual-targeted cationic liposomes modified with hyaluronic acid and folic acid deliver siRNA Bcl-2 in the treatment of cervical cancer

**Yao Tong**

Soochow University

**Wen-jun Wan**

Soochow University

**Han Yang**

Yangtze River Pharmaceutical Group

**Yu Wang**

Soochow University

**Dan-dan Wang**

Soochow University

**Yang Liu**

Soochow University

**Beng-gang You**

Soochow University

**Xue-nong Zhang** (✉ [zhangxuenong@163.com](mailto:zhangxuenong@163.com))

Soochow University

---

## Research

**Keywords:** dual-targeted, liposome, siRNA, Bcl-2, cervical cancer

**Posted Date:** April 7th, 2020

**DOI:** <https://doi.org/10.21203/rs.3.rs-20688/v1>

**License:** © ⓘ This work is licensed under a Creative Commons Attribution 4.0 International License.

[Read Full License](#)

---

# Abstract

**Background:** Gene therapy has attracted widespread attention as a potential method of treating some autoimmune diseases, genetic diseases and cancer. It is critical to discover a new nanocarrier for the effectiveness of gene therapy. Reportedly, the dual-targeted nano-delivery system as a novel strategy could improve targeting efficiency and deliver more drugs or genes to tumor sites over current single-targeted nano-delivery delivery system.

**Methods:** We synthesized and characterized the hyaluronic acid (HA)-folic acid (FA) polymer, and then prepared the cationic liposomes by ultrasonic dispersion . The liposome was coated with HA-FA to obtain HA-FA-Lip nanoparticles. HA-FA-Lip formed complexes with siRNA Bcl-2 (siBcl-2) through electrostatic adsorption for delivering siBcl-2 to the tumor site.

**Results:** HA-FA-Lip showed stronger tumor accumulation and better targeting efficiency than HA-lip. Meanwhile, HA-FA-Lip delivered more siBcl-2 to tumor cells and played a role in down-regulating Bcl protein levels, thus inducing obvious apoptosis.

**Conclusions:** As a new type of dual-targeted drug delivery system, HA-FA-Lip was expected to be an effective nanocarrier with high transfection efficiency and good biocompatibility.

# Background

Cervical cancer is one of the most common gynecological malignancies in the world [1]. Traditional surgical treatment and chemotherapy for cervical cancer have serious side effects and could not achieve the desired effect [2]. Gene therapy refers to a biological treatment method that uses foreign gene transfer technology to introduce foreign genes into normal target cells to repair or correct genetic abnormalities and defects [3,4]. RNA interference(RNAi)technology has become a trend in the development of tumor treatment due to its safety, effectiveness and specificity [5]. And it has been reported that small interfering RNA (siRNA) could trigger the degradation of homologous mRNA and down-regulate the expression of the target protein [6]. Many studies have shown that some important signaling pathways such as apoptotic play a key role in the occurrence and development of tumors [7–9]. Researchers have also found that the Bcl-2 protein as a major anti-apoptotic member of Bcl-2 family proteins is closely related to apoptotic pathway[10,11]. Tumor cells avoid apoptosis by overexpressing Bcl-2 protein, which is helpful for tumorigenesis and metastasis [12,13]. Therefore, the use of RNAi technology to reduce the expression levels of Bcl-2 protein would induce apoptosis of cancer cells and have a good therapeutic effect [15–17].

However, due to the hydrophilicity and instability of siRNA, how to efficiently deliver to the tumor site becomes a challenge [18]. Cationic liposomes which is a commonly used gene vector with high transfection efficiency, are able to adsorb siRNA and protect it from enzymatic hydrolysis [19]. However, the positive charge of cationic liposomes makes it poor in stability during blood circulation and causes systemic toxicity [20–22]. Therefore, the surface of cationic liposomes needs to be modified to overcome these obstacles [23, 24]. For example, the modification of PEG has been shown to be less easily

recognized by the reticuloendothelial system and prolong the half-life [25]. In order to achieve higher targeting efficiency, liposomes usually modify ligands on their surface and interact with specific receptors on the target cells to promote the internalization of liposomes [26–28]. Currently, the receptors commonly used that are overexpressed on the surface of tumor cells include hyaluronic acid receptor, folic acid receptor, integrin receptor and others. [29–31].

Reportedly, the dual-ligand modified liposomes are better than single-ligand modified liposomes for delivering drugs to tumor sites and increasing their accumulation in tumor sites [32–34]. In this study, we covalently linked hyaluronic acid with folic acid to form a polymer (HA-FA), and the cationic liposomes were coated with HA-FA polymer through electrostatic adsorption to construct a dual-targeted nanocarrier (HA-FA-Lip), which shielded positive charges and reduces cytotoxicity (Fig. 1). Then HA-FA-Lip bound siBcl-2 completely, remained stable in the blood circulation and accumulated in tumor sites through the EPR effect and the active targeting capability by dual-ligand modification. The HA-FA polymer targeted folate receptors and CD44 receptors on the surface of HeLa cells and increased the cellular uptake of nanoparticles. Finally, siBcl-2 played an important role in down-regulating Bcl-2 protein expression, induced apoptosis of cancer cells and showed excellent treatment efficiency.

## Materials

Folate acid was purchased from Shanghai Qiangshuo Chemical Reagent Co., Ltd (Shanghai, China). Hyaluronic acid and formamide were provided from Anaiji Chemical Co., Ltd (Shanghai, China). Dimethyl sulfoxide (DMSO), chloroform ( $\text{CHCl}_3$ ), methanol ( $\text{CH}_3\text{OH}$ ), and cholesterol (Chol) were from Sinopharm Chemical Reagent Co., Ltd. 2,3-Dioleoyl-propyl-trimethylamine (DOTAP) and Dioleoyl ethanolamine (DOPE) were from Corden Pharma (Switzerland). siRNA targeting Bcl-2 (sense sequence: 5'-ACG UGA CAC GUU CGG AGA ATT-3'), and siRNA-NC or siRNA-NC labeled with FAM (siRNA<sup>FAM</sup>) were obtained from GenePharma Co., Ltd (Shanghai, China). Fetal bovine serum (FBS) was provided by Hangzhou Sijiqing Engineering Materials Co., Ltd (Hangzhou, China). Bovine serum albumin (BSA), agarose, Gel Red, 6 × DNA loading buffer and bicinchoninic acid (BCA) protein assay kit were provided by Biyuntian Biotechnology Co., Ltd (Shanghai, China). 3-(4,5-Dimethyl-2-thiazolyl)-2,5-diphenyl-2H-tetrazolium bromide (MTT) was provided from Sigma-Aldrich (St. Louis, Missouri, USA).

HeLa cells (human cervical cancer) were provided by Soochow University (Suzhou, China) and cultured in DMEM with 10% (v/v) fetal bovine serum and 1% (v/v) penicillin – streptomycin solution at 37 °C in a humidified atmosphere containing 5%  $\text{CO}_2$ .

Femal nude mice (age of 4 – 6 w) were obtained from the Experimental Animal Center of Soochow University (Suzhou, China). All mice are housed in an environment that complies with the National Institutes of Health guidelines for the care and use of laboratory animals. All animal procedures were performed in accordance with protocols approved by the Institutional Animal Care and Use Committee.

## Methods

## **Synthesis and characterization of HA-FA polymer**

FA was added in dimethyl sulfoxide and stirred to dissolve completely. Then dicyclohexylcarbodiimide (DCC) and N-hydroxysuccinimide (NHS) were added to the FA solutions and stirred at 30 °C for 5 h, and the precipitate was removed by filtration. Then HA was dissolved in formamide, the previously prepared FA solution was added dropwise to the HA solution. The mixture was stirred constantly at 40 °C for 48 h and protected from light. The liquid obtained after filtration was dialyzed (MWCO = 3000) in deionized water for 48 h and lyophilized to obtain the final product (HA-FA). The structure of HA-FA was studied through <sup>1</sup>H nuclear magnetic resonance (<sup>1</sup>H NMR) spectroscopy (400 MHz, Varian, Palo Alto, CA, USA) and Fourier transform-infrared (FT-IR) spectrometry (Varian, Palo Alto, CA, USA)

## **Preparation and characterization of Lip, HA-Lip and HA-FA-Lip**

The cationic liposomes (Lip) are prepared by ultrasonic dispersion using DOTAP, DOPE and cholesterol as raw materials. Then, Lip was slowly dripped into the HA or HA-FA solution (1 mg/mL) according to the volume ratio of 1: 1. The mixture was continuously stirred for 15min to obtain HA-Lip or HA-FA-Lip. The particle distribution of and zeta potential of black Lip, HA-Lip and HA-FA-Lip was observed by dynamic light scattering (DLS) method (Zetasizer Nano ZSP; Malvern Instruments, Ltd.). The morphology of HA-FA-Lip was studied by a transmission electron microscope(TEM) instrument (JEOL Ltd., Japan)

## **The adsorption efficiency of Lip, HA-Lip, HA-FA-Lip on siRNA**

Garose gel electrophoresis was used to investigate the ability of Lip to adsorb siRNA. Agarose gel (1.5%) was prepared, then lip was mixed with siRNA solution at nitrogen/phosphate (N/P) ratios of 0: 1, 1: 1, 2: 1, 4: 1, 6: 1, and 8: 1. Lip was adsorbed to siRNA through electrostatic adsorption. We took 10 μL of Lip/siRNA complexes with different N/P ratios, added 2 μL of DNA loading buffer (6×) to prepare the mixture. Then, the mixture was vortexed and loaded in 1.5% agarose gel. The optimal N/P ratio was obtained by image analysis. Lip/siRNA was prepared according to the optimal N/P ratio ( N/P = 6), and then dropped into the HA and HA-FA solutions slowly, and mixed by vortexing, equilibrated at room temperature for 15 min to obtain HA-Lip/siRNA and HA-FA-Lip/siRNA. We detected the adsorption of siRNA on different liposomes through the same method.

## **Serum stability and protein adsorption**

The serum stability and protein adsorption rate of nanoparticles are very important for the stable delivery of nanoparticles to tumor sites. To observe the serum stability of diferent liposomes, we added 100 μL of Lip, HA-Lip or HA-FA-Lip solutions into a 96-well plate and incubated with 100μL of fetal bovine serum (FBS) at 37 °C. The absorbance values of each well were measured at 630 nm via a full-wavelength microplate reader at predesigned time points. Saline (0.9%) was set as negative control. The relative turbidity was obtained by calculating the ratio of absorbance of each sample group and saline group at each time point.

To detect protein adsorption, we mixed blank Lip, HA-Lip, or HA-FA-Lip nanoparticle solutions (each 1 mg/mL) with BSA solution (1mg/ml) in equal amounts, and incubated the mixture at 37 °C for 6 h. After that, the mixture was centrifuged at 12000 rpm and 4 ° C for 15 minutes. We took 20 μL of the supernatant from each group and added it to a 96-well plate. The protein concentration of each group was measured by the BCA kit. The protein adsorption rate (PAR%) was calculated as follows:  $Par\% = (C_0 - C_1) / C_0$

Among them:  $C_0$  and  $C_1$  are the protein concentration of the supernatant of the control group and the sample group after centrifugation, respectively.

### **Cytotoxicity by MTT assay**

The MTT assay was employed to detect the cytotoxicity of various blank liposomes *in vitro*. HeLa cells in the logarithmic growth phase were seeded into 96-well plates (5000 cells/well) and cultured for 24 h. The cells were cultured in 200 μL of fresh medium containing various concentrations of blank Lip, HA-Lip and HA-FA-Lip respectively for 24 h. After that, MTT (20 μL, 5mg/mL) were added to each well. Four hours later, the supernatant was discarded, and 150μL of DMSO were added to dissolve formazan in the 96-well plates. We shook them on a microplate shaker for 15 minutes and measured the absorbance of each well at 570 nm with a full-wavelength microplate reader. Cell viability of each group was calculated using the following equation:  $Cell\ viability = (A_{570(sample)} - A_0) / (A_{570(control)} - A_0) \times 100\%$ , where  $A_{570(sample)}$  and  $A_{570(control)}$  represent the absorbance of cells group treated with different formulations and the non-treated cells group, respectively.  $A_0$  represents medium-only group.

### **Cellular uptake assay**

For quantitative evaluation, the ability of HeLa cells to internalize siRNA<sup>FAM</sup> was investigated by flow cytometry. HeLa cells in the logarithmic growth phase were seeded in 6-well plates ( $1 \times 10^6$  per well) and cultured for 24 h. After treatment with Lip/siRNA<sup>FAM</sup>, HA-Lip/siRNA<sup>FAM</sup>, or HA-FA-Lip/siRNA<sup>FAM</sup> for 4h, cells were collected and washed with PBS several times, and finally the cells were resuspended with PBS. The final concentration of siRNA<sup>FAM</sup> in each group was 100 nM. The FAM fluorescence signal in the cells was analyzed by a flow cytometer (FC500, Beckman Coulter, USA).

In order to observe the localization of siRNA<sup>FAM</sup> after being taken up by HeLa cells, the images were observed by confocal laser scanning microscopy (CLSM) (ZEISS, Germany). HeLa cells in the logarithmic growth phase were seeded in glass-bottomed dishes ( $1 \times 10^6$  cells/ dish) and cultured for 24 h. Briefly, cells were incubated with Lip/siRNA<sup>FAM</sup>, HA-Lip/siRNA<sup>FAM</sup>, and HA-FA-Lip/siRNA<sup>FAM</sup> for 2 h or 4h. After that, the cells nuclei were stained with Hoechst 33258 (10 μg/ml), fixed with 4% paraformaldehyde and rinsed with PBS several times. Then cells were added with an appropriate amount of anti-fluorescent quencher, covered with coverslips, and we obtained images by CLSM.

### **Transfection efficiency of siBcl-2 and cell apoptosis in vitro**

It has been reported that siRNA could down-regulate the expression of target protein in cells [15]. HeLa cells in logarithmic growth phase were seeded into 6-well plates and cultured for 24 h, then treated with Lip/siBcl-2, HA-Lip/siBcl-2 or HA-FA-Lip/siBcl-2 for 6h. The final concentration of siBcl-2 was 100 nM per well. After replacing the serum-free medium with the serum-containing medium, the cells were further cultured for 48h. Then we extracted the protein and performed Western blot assay to investigate the expression of Bcl-2 protein in different groups. The gray value of each group of protein bands was analyzed with Image J software and statistical analysis was performed.

We also found that the concentration of siRNA and the incubation time after treating siBcl-2 had some effects on the transfection efficiency of HA-FA-Lip/siBcl-2. HeLa cells were seeded and cultured in the same way as before. The cells were treated with HA-FA-Lip/siBcl-2, containing different concentrations of siBcl-2 for 6h. The final concentration of siBcl-2 was 100 nM or 200nM per well. After treating with different formulations, the drug-containing medium was changed to fresh serum-containing medium. In order to observe the optimal transfection time, the cells were cultured for 24h or 48 h, protein extraction and Western blot assay were performed as before.

The changes in Bcl-2 protein levels maybe have a great effect on tumor cell apoptosis[9]. HeLa cells in the logarithmic growth phase were seeded in 96-well plates (5000 cells /well) and cultured for 24 h. The medium was changed to a serum-free medium, then Lip/siBcl-2, HA-Lip/ siBcl-2, and HA-FA-Lip/siBcl-2 were added, respectively. And the final concentration of siBcl-2 was 100 nM per well. After 6 hours, the drug-containing medium was changed to a serum-containing medium, and transfection was continued for 48 h. We removed the cell culture medium, added 100  $\mu$ L 4% paraformaldehyde fixative solution to each well. The cells were stained with the TUNEL/TdT-mediated dUTP nick end labeling/apoptosis detection kit, and images were captured by CLSM.

### **Targeting evaluation of nanoparticles in vivo**

Each nude mouse was inoculated with 0.1 mL of cell suspension ( $10^5$  cells/ml) on the right side. When the tumor volume increased to  $100 \pm 20$  mm<sup>3</sup>, we obtained the tumor-bearing mice for our study. Dir was dissolved with organic solvent, then added to the prepared Lip for probe-ultrasound. The organic solvent was rotated and evaporated to obtain Lip/Dir. The concentration of Dir was 1 mg/mL. HA-Lip/Dir and HA-FA-Lip/Dir was prepared according to the same method. Nude mice were injected with 0.1 mL of HA-Lip/Dir and HA-FA-Lip/Dir in the tail vein. After administration of 12, 24, and 48 h, fluorescence intensity and bio-distribution of Dir in each group were investigated by the IVIS<sup>®</sup> Spectrum imaging system (Caliper Life Sciences). Then the mice were sacrificed, and the heart, liver, spleen, lung, kidney and tumor were dissected out to examine the fluorescence intensity. Fluorescence intensity was determined via region-of-interest (ROI) analysis.

### **In vivo pharmacodynamics and safety of nanoparticles**

Subcutaneous tumor-bearing nude mice models were produced by the methods previously described. When the tumors grew to about 100 mm<sup>3</sup>, they were randomly divided into three groups, which were

administered with 100ul of saline, HA-Lip/siBcl-2, and HA-FA-Lip/siBcl-2, respectively. siBcl-2 was at a concentration of 0.33 mg/kg in all groups. Treatments were performed at days 1, 3, 5, and 7. The mice were sacrificed after the last treatment, and tumor tissues and main organs were stripped for subsequent experiments.

The Bcl-2 protein expression in tumor tissues were detected by an important mean of Western blot analysis. We put an appropriate amount of tumor tissue in an EP tube, added radioimmunoprecipitation assay (RIPA) buffer containing 1 mM Phenylmethanesulfonyl fluoride (PMSF). The tumor tissue was cut with small scissors, sonicated and then lysed on ice. After centrifugation, the supernatant was transferred to a clean EP tubes to obtain protein solution. Western blot assay were performed according to the previously described procedures. Hematoxylin–eosin (H&E) staining and TUNEL staining were used to further study the safety of nanoparticles in vivo and cell apoptosis in tumor tissues.

### Statistical analysis

All the experimental data were represented as mean  $\pm$  standard deviation (SD). Student's test or one-way analysis of variance was performed for Statistical analysis. Statistical significance was defined as \*  $p < 0.05$ , \*\*  $p < 0.01$  and \*\*\* $p < 0.001$ .

## Results

### The characterization of HA-FA polymer

The synthesis of HA-FA polymer follows the route shown in the **Fig.2A**. The HA-FA polymer was dissolved in  $D_2O$  and its structure was characterized by  $^1H$ -NMR. From the results of the spectrum (**Fig.2B**), the characteristic peaks of HA appeared at  $\delta = 6.6$ - $8.6$  ppm, and the characteristic absorption peaks of FA and HA were all visible along the spectrum of the HA-FA polymer. The grafting rate of HA was calculated to 44.8% by peak area integration .

As shown in **Fig.2C**, HA-FA showed that the stretching vibration peaks of ester bond  $C=O$  at  $1565\text{ cm}^{-1}$ , the enhancement of the stretching vibration peaks of carboxyl  $-COOH$  at  $3277\text{ cm}^{-1}$  and the amino ( $-NH_2$ ) at  $1606\text{ cm}^{-1}$ . It was proved that FA has been successfully grafted onto HA. Therefore, the results of  $^1H$ -NMR and FT-IR both indicated the successful synthesis of HA-FA. HA-FA would be used as a polymer that double-targets hyaluronic acid receptor and folic acid receptor.

### The characterization of Lip, HA-Lip and HA-FA-Lip

The size distribution of different liposomes was shown in **Fig.3A**. It was revealed that Lip has a uniform size of  $67.6\text{ nm}$  (PDI = 0.222) and showed a very significant increase in size with HA-FA coating. The particle sizes of HA-Lip and HA-FA-Lip were around  $130.6\text{ nm}$  (PDI = 0.185) and  $125.6\text{ nm}$  (PDI = 0.105). The zeta potential also changed from positive to negative (**Fig.3B**). The potential of Lip was around  $+40.8\text{ mv}$  and showed strong positive charge, while HA-lip became around  $-22.6\text{ mv}$  and HA-FA-Lip became

around -22.4 mv. These changes in particle size and zeta potential proved that HA and HA-FA had been successfully coated the surface of cationic Lip through electrostatic adsorption. Notably, both HA-lip and HA-FA-Lip were stable and had good dispersibility. The morphology of HA-FA-lip was round and uniformly distributed (**Fig.3C**). The diameter of HA-FA-lip was about 120nm, which was consistent with the results of DLS. It was likely that HA-FA-Lip could not only accumulate in tumor sites through the EPR effect because they have an appropriate nanosize, but also can target tumor sites through the dual receptors of hyaluronic acid and folict acid.

### **The adsorption efficiency of Lip, HA-Lip, HA-FA-Lip on siRNA**

As was evident from **Fig.3D**, the band of free siRNA (N/P = 0) was bright and with the increase of N/P ratio, the brightness of band gradually decreased until it disappeared almost completely at N/P = 6. This indicated that siRNA had been completely adsorbed by Lip. In subsequent experiments, the optimal N/P ratio (N/P=6) was used to prepare Lip/siRNA. And Lip/siRNA, HA-Lip/siRNA and HA-FA-Lip/siRNA did not show obvious bright bands (**Fig.3E**), which proved that the coating of HA and HA-FA would not cause the leakage of siRNA.

### **Serum stability and protein adsorption**

Reportedly, negatively charged nanoparticles have better serum stability during blood circulation [9]. Notably, this showed that that the turbidity of the Lip group increased significantly with time after incubation with fetal bovine serum (**Fig.4A**). Because the uncoated Lip had a strong positive charge, it interacted strongly with serum. However, the interaction of HA-Lip or HA-FA-Lip with serum after coating was significantly reduced, and there was no significant change with time. Besides, the positively charged Liposome easily adsorbs the negatively charged BSA. It appeared that the protein adsorption rate of Lip was about 42.5% (**Fig.4B**). After HA and HA-FA coating, the protein adsorption rate decreased to 9.4% and 7.6%, respectively. It was suggested that HA or HA-FA coating would reduce serum-induced aggregation and reduce the adsorption of protein to improve the stability of nanocarrier during the blood circulation in vivo. It was also beneficial for HA-FA-Lip to maintain a relatively stable particle size in the circulation, so as to facilitate the subsequent EPR effect.

### **Cell cytotoxicity of blank liposome**

The MTT results showed that the cell survival rate of the Lip group was only 61% when the concentration of blank liposomes was 62.5  $\mu\text{g}/\text{mL}$ , while the cell survival rate of the HA-Lip group and the HA-FA-Lip group were higher than 90% (**Fig.4C**). Additionally, HA-Lip and HA-FA-Lip had no significant toxicity in the concentration range of 0-250  $\mu\text{g}/\text{ml}$ , which proved good safety. When the concentration was greater than 31.25 $\mu\text{g}/\text{ml}$ , the cell survival rate of Lip group decreased significantly with the increase of concentration. The result demonstrated that HA-Lip and HA-FA-Lip had less toxicity and good biocompatibility. The coating of HA and HA-FA could be able to significantly reduce the cytotoxicity of the cationic nanocarrier.

### **Cellular uptake assay**

When the nanoparticles reach the tumor site, whether the nanoparticles are effectively taken up by the cells is the key to whether the loaded drug can have a therapeutic effect. We quantified the cellular uptake of siRNA by flow cytometry. Results showed that the fluorescence intensity of HA-FA-Lip/siRNA<sup>FAM</sup> was 2.1 times that of Lip/siRNA<sup>FAM</sup> group and 1.8 times that of HA-Lip/siRNA<sup>FAM</sup> (Fig.5A and B). This proved that HA-FA-coated liposomes had the ability to target the hyaluronic acid and folic acid receptors on the surface of tumor cells, which significantly increased the internalization of HA-FA-Lip/siRNA<sup>FAM</sup> by Hela cells, allowing more siRNA to enter the cells. We also found that the uptake of the Lip/siRNA<sup>FAM</sup> group and HA-Lip/siRNA<sup>FAM</sup> were not significantly different. It might be due to that the positive charge of Lip was favorable for cellular uptake. However, the endocytosis in the HA-Lip/siRNA<sup>FAM</sup> group was mediated by recognition and binding between single ligand and receptor.

The liposomes we prepared contained DOPE, which could promote membrane fusion and increase the instability of the lipid membrane, so the complex was more easily released into the cytoplasm. The images showed that liposomes carried siRNA into cells, and siRNA<sup>FAM</sup> was mainly localized in the cell cytoplasm (Fig5C). The stronger green fluorescence of the siRNA<sup>FAM</sup> was observed in the cells at 4 h. It was likely that the cellular uptake of siRNA significantly increased with time. And the co-localization of siRNA in HA-FA-Lip/siRNA group was significantly increased compared with Lip/siRNA group and HA-Lip/siRNA group at 2h or 4h, which was consistent with the results of flow cytometry.

### Transfection efficiency of siBcl-2 and cell apoptosis in vitro

It has been reported that siRNA forms an RNA induced silencing complex (RISC), which degrades the mRNA of target genes in cells and silences the expression of target proteins [6]. Compared with Lip/siRNA<sup>FAM</sup>, HA-Lip/siRNA<sup>FAM</sup> showed almost equivalent transfection efficiency (Fig.6A). This may be caused by the similar results of cellular uptake. The down-regulating expression of Bcl-2 protein in the HA-FA-Lip/siBcl-2 group was better than the other two groups. And the efficiency of silencing Bcl-2 protein was about 77% at a concentration of 200 nM and a transfection time of 48 h (Fig.6B). And the silencing effect of siBcl-2 on Bcl2 protein was obviously time and concentration dependent. Considering that when the concentration of siRNA was high, more liposomes were needed to prevent leakage. But according to MTT results, the cell toxicity of liposomes would also increase. Therefore, the HA-FA-Lip/siBcl-2 group had shown a good silencing effect and very low cytotoxicity when the siRNA concentration was set to 100 nM.

Meanwhile, Bcl-2 protein plays a important role in inhibiting cell apoptosis in vivo. The images demonstrated that the cells treated with HA-FA-Lip/siBcl-2 showed more intense fluorescent staining spots (Fig. 6C). The cell apoptosis induced by HA-FA-Lip/siBcl-2<sup>FAM</sup> was higher than that of Lip/siBcl-2<sup>FAM</sup> group and HA-Lip/siBcl-2<sup>FAM</sup> group. These observations suggested that the coating of dual-targeted HA-FA increased the internalization of the liposomes by Hela cells and enhanced the transfection efficiency of the cationic nanocarrier in vitro. And more siBcl-2 entered the cells and had the effect of inducing obvious apoptosis of cancer cells.

## Targeting evaluation of nanoparticles in vivo

The two groups of nanoparticles have a suitable nanosize between 100-200nm, which could aggregate to the tumor site through the EPR effect. By monitoring the distribution of DiR fluorescence in tumor-bearing mice, the tumor site in the HA-FA-Lip/Dir group had obvious fluorescence at 12h (**Fig.7A**). But in the HA-Lip/Dir group, fluorescence appeared in the tumor site at 24 h, and it may be due to metabolism that the fluorescence of the tumor site slightly weakened at 48h. But in the HA-FA-Lip/Dir group, more nanoparticles aggregated at the tumor site at 48h, and the accumulation of DiR-loaded nanoparticles in tumor areas increased with time. The fluorescence intensity of the tumor site in the HA-FA-Lip/Dir group was significantly higher than that in the HA-Lip group (**Fig.7B**). At the same time, there was also obvious fluorescence in mouse liver, which caused by phagocytosis of the reticuloendothelial system. It was evident that dual-targeted HA-FA-Lip/Dir group had stronger fluorescence in the tumor area than single-targeted HA-Lip/Dir group, and showed higher accumulation in tumor sites. This demonstrated that HA-FA-coated liposomes have better tumor targeting than HA-coated liposomes, and delivered more siBcl-2 to tumor sites to exert therapeutic effect.

## Gene silencing assessment in vitro

We injected tumor-bearing mice with siBcl-2-loaded nanoparticles, and extracted proteins from tumor tissues for Western Blot assay. As shown in **Fig.8A**, both HA-FA-Lip and HA-Lip significantly downregulated the expression of Bcl-2 protein in tumor tissues. Compared with the HA-Lip/siBcl-2 group, the HA-FA-Lip/siBcl-2 group has a higher silencing efficiency on Bcl-2 protein of tumor tissues. Cell apoptosis in tumor tissues was analyzed via TUNEL assay. Furthermore, the results of TUNEL staining in the HA-FA-Lip/siBcl-2 group showed more red fluorescent spots, which represented a larger proportion of apoptotic tumor cells. After treatment, **H&E** staining was performed on the mice in each group. The nanoparticles in all groups did not cause damage to the main organs, and had good safety in vivo.

## Discussion

The approach of modifying the surface of liposomes with some specific ligands plays an important role in targeted drug delivery systems[35]. Due to the shortcomings of traditional single-ligand modified liposomes, such as limited targeting efficiency and low cellular uptake, many researchers continue to explore the use of two or more different ligands to modify liposomes [36,37]. In our study, we successfully prepared HA-FA-Lip nanoparticles, and it has been proven to achieve the effective delivery in vivo, which might be due to the EPR effect and the active targeting capability by dual-ligand modification. The dual-targeted HA-FA-Lip interacted with CD44 and folate receptors on the cell surface and increased the internalization of nanoparticles through dual-receptor mediated endocytosis. However, the HA-Lip had a single target and only binded to the CD44 receptor, so its interaction with the receptor was limited, and its localization effect was less precise than HA-FA-Lip. We suspected it might be that dual-ligand modification has the advantage of increasing the chance of liposomes to adhere to target cells, thereby enhancing targeting accuracy and efficiency.

Therefore, the dual-targeted nanocarrier provided a novel strategy to improve targeting efficiency over current single-targeted drug delivery system, and the results demonstrated the utility of these dual or multiple ligand modification in this study. These different ligands could play a synergistic or additive role, so it will be possible to customize nanocarriers containing dual or multiple targeting ligands to suit the characteristics of targeted tissues and allow patients to receive specific treatments in the future. We look forward to more discovery and application of those specific ligands, and the more ingenious combination of these modified ligands will help us to build more novel targeted drug delivery system.

## Conclusion

In this study, we have successfully prepared the HA-FA polymer with good water solubility and used it to coat Lip to obtain HA-FA-Lip. These results showed that the particle size of HA-FA-Lip was about 125.6 nm and homogeneously distributed. And the shape of nanoparticles was round and uniform. The coating of HA and HA-FA shielded the positive charge of Lip, improved the safety of the nanocarrier and reduce the cell cytotoxicity. Compared with HA-Lip, dual-targeted HA-FA-Lip increased intracellular uptake of the nanoparticles through dual-receptor mediated endocytosis pathway. It was worth noting that HA-FA-Lip show stronger tumor accumulation and better tumor targeting efficiency than HA-lip. Meanwhile, we found that HA-FA-Lip efficiently delivered siBcl-2 to tumor cells and played a role in down-regulating Bcl protein levels, thus inducing obvious apoptosis. Moreover, no significant pathological changes occurred in the main organs of the mice in each group after treatment. In summary, the HA-FA-Lip prepared in this study could be used as a new type of nanovehicles with high transfection efficiency and good biocompatibility.

## Abbreviations

HA: hyaluronic acid; FA: folic acid; DMSO: Dimethyl sulfoxide; DOTAP: 2,3-Dioleoyl-propyl-trimethylamine ; DOPE: Dioleoylethanolamine; FBS: Fetal bovine serum; BSA: Bovine serum albumin.

## Declarations

### Authors' contributions

YT and WJW performed the experiments, analyzed the data and drafted the manuscript. HY discussed the data and gave some advice. YW was involved in an animal experiment, DDW, YL, BGY assisted in the analysis of biological data. XNZ directed the experiment and supervised the work. All authors read and approved the final manuscript.

### Author details

a. Department of Pharmaceutics, College of Pharmaceutical Sciences, Soochow University, Suzhou 215123, People's Republic of China

b. Yangtze River Pharmaceutical Group Jiangsu coastal Pharmaceutical Co., Ltd, Suzhou 215211, People's Republic of China

## Acknowledgements

This work was supported by the National Natural Science Foundation projects of China (Nos. 81571788 and 81773183), post graduate research & practice innovation program of Jiangsu Province (No. KYCX19\_1973) and Priority Academic Program Development of Jiangsu Higher Education Institutions (PAPD).

## Competing interests

The authors declare that they have no competing interests.

## Data sharing

Data sharing is not applicable to this article, as no datasets were generated or analyzed during the current study.

## Ethics approval, consent to participate, and publication

This submission reports that no data were collected from humans, and this study did not involve any individual person's data in any form. All mice are housed in an environment that complies with the National Institutes of Health guidelines for the care and use of laboratory animals. All animal procedures were performed in accordance with protocols approved by the Institutional Animal Care and Use Committee.

## Funding

This work was supported by the National Natural Science Foundation projects of China (Nos. 81571788 and 81773183), post graduate research & practice innovation program of Jiangsu Province (No. KYCX19\_1973) and Priority Academic Program Development of Jiangsu Higher Education Institutions (PAPD)

## References

- [1] Biaoxue R, Xiguang C, Hua L, et al. Stathmin-dependent molecular targeting therapy for malignant tumor: the latest 5 years' discoveries and developments. *J Transl Med.* 2016;14(1):279-97.
- [2] Rong B, Cai X, Yang S, et al. EphA2-Dependent Molecular Targeting Therapy for Malignant Tumors. *Curr Cancer Drug Targets.* 2011;11(9):1082-97.
- [3] Wirth T, Parker N, Ylä-Herttuala S. History of gene therapy. *Gene.* 2013;525(2):162-9.

- [4] Ginn SL, Amaya AK, Alexander IE, et al. Gene therapy clinical trials worldwide to 2017: An update. *J Gene Med*. 2018;20(5):e3015.
- [5] Fire A, Xu SQ, Montgomery MK, et al. Potent and specific genetic interference by double-stranded RNA in *Caenorhabditis elegans*. *Nature*. 1998;391(6669): 806-11.
- [6] Patil, Y, Panyam, J. Polymeric nanoparticles for siRNA delivery and gene silencing. *Int J Pharm*. 2009;367(1–2):195–203.
- [7] Conde J, Tian F, Hernández Y, et al. In vivo tumor targeting via nanoparticle-mediated therapeutic siRNA coupled to inflammatory response in lung cancer mouse models. *Biomaterials*. 2013;34(31):7744-53.
- [8] Zhang D, Li B, Shi J, et al. Suppression of Tumor Growth and Metastasis by Simultaneously Blocking Vascular Endothelial Growth Factor (VEGF)-A and VEGF-C with a Receptor-Immunoglobulin Fusion Protein. *Cancer Res*. 2010;70(6):2495-503.
- [9] Li F, Wang Y, Chen WL, et al. Co-delivery of VEGF siRNA and etoposide for enhanced anti-angiogenesis and anti-proliferation effect via multi-functional nanoparticles for orthotopic non-small cell lung cancer treatment. *Theranostics*. 2019;9(20): 5886-5898..
- [10] Oltersdorf T, Elmore SW, Shoemaker AR, et al. An inhibitor of Bcl-2 family proteins induces regression of solid tumours. *Nature*. 2005;435(7042): 677-81.
- [11] Yu S, Gong LS, Li NF, et al. **Galangin (GG) combined with cisplatin (DDP) to suppress human lung cancer by inhibition of STAT3-regulated NF- $\kappa$ B and Bcl-2/Bax signaling pathways.** *Biomed Pharmacother*. 2018; 97:213-224.
- [12] Han SZ, Liu HX, Yang LQ, Cui LD, Xu Y. **Piperine (PP) enhanced mitomycin-C (MMC) therapy of human cervical cancer through suppressing Bcl-2 signaling pathway via inactivating STAT3/NF- $\kappa$ B.** *Biomed Pharmacother*. 2017;96:1403-1410
- [12] Lee SJ, Yook S, Yhee JY, et al. **Co-delivery of VEGF and Bcl-2 dual-targeted siRNA polymer using a single nanoparticle for synergistic anti-cancer effects in vivo.** *J Control Release*. 2015; 220: 631-641
- [14] Wu H, Medeiros LJ, Young KH. **Apoptosis signaling and BCL-2 pathways provide opportunities for novel targeted therapeutic strategies in hematologic malignances.** *Blood Rev*. 2018; 32(1):8-28
- [15] Li JM, Zhang W, Su H, et al. **Reversal of multidrug resistance in MCF-7/Adr cells by codelivery of doxorubicin and BCL2 siRNA using a folic acid-conjugated polyethylenimine hydroxypropyl- $\beta$ -cyclodextrin nanocarrier.** *Int J Nanomedicine*. 2015;10:3147-62.
- [16] Wu D, Yang J, Xing Z, et al. **Phenylboronic acid-functionalized polyamidoamine-mediated Bcl-2 siRNA delivery for inhibiting the cell proliferation.** *Colloids Surf B Biointerfaces*. 2016;146:318-325

- [17] Qian J, Xu M, Suo A, et al. Folate-decorated hydrophilic three-arm star-block terpolymer as a novel nanovehicle for targeted co-delivery of doxorubicin and Bcl-2 siRNA in breast cancer therapy. *Acta Biomater.* 2015;15:102-16.
- [18] Lee, SJ, KimMJ, Kwon IC, RobertsTM. Delivery strategies and potential targets for siRNA in major cancer types. *Adv Drug Deliv Rev.* 2016;104:2-15.
- [19] Allen, TM, Cullis, PR. Liposomal drug delivery systems: From concept to clinical applications. *Adv Drug Deliv Rev.* 2013;65(1):36-48
- [20] Palchetti S, Pozzi D, Marchini C, et al. Manipulation of lipoplex concentration at the cell surface boosts transfection efficiency in hard-to-transfect cells. 2017;13(2): 681-91.
- [21] Shim G, Han SE, Yu YH, Lee S, Lee HY, Oh YK. Trilysinoyl oleylamide-based cationic liposomes for systemic co-delivery of siRNA and an anticancer drug. *J Control Release.* 2011;155:60-6.
- [22] Barenholz Y. Liposome application: problems and prospects. *Curr Opin Colloid Interface Sci.* 2001;6:66–77
- [23] Yang ZZ, Li JQ, Wang ZZ, Dong DW, Qi XR. Tumor-targeting dual peptides-modified cationic liposomes for delivery of siRNA and docetaxel to gliomas. *Biomaterials.* 2014; 35:5226-39.
- [24] Abu LA, Okada T, Doi Y, Ichihara M, Ishida T, Kiwada H. Combination therapy with metronomic s-1 dosing and oxaliplatin-containing peg-coated cationic liposomes in a murine colorectal tumor model: synergy or antagonism?. *Int J Pharm.* 2012; 426: 263-70.
- [25] Kibria G, Hatakeyama H, Ohga N, et al. Dual-ligand modification of PEGylated liposomes shows better cell selectivity and efficient gene delivery. *J Control Release.* 2011;153(2):141-148.
- [26] Takara K, Hatakeyama H, Ohga N, et al. Design of a dual-ligand system using a specific ligand and cell penetrating peptide, resulting in a synergistic effect on selectivity and cellular uptake. *In J Pharm.* 2010,153(2):141-148.
- [27] Sutton D, Nasongkla N, Blanco E, et al. Functionalized micellar systems for cancer targeted drug delivery. *Pharm Res.* 2007;24(6):1029-46. 2007
- [28] Torchilin V. Targeted polymeric micelles for delivery of poorly soluble drugs. *Cell Mol Life Sci.* 2004;61(19-20):2549-59.
- [29] Zhang L, Gao S, Zhang F, et al. Activatable hyaluronic acid nanoparticle as a theranostic agent for optical/photoacoustic image-guided photothermal therapy. *ACS Nano.* 2014;8(12):12250-8.
- [30] Liu Y, Dai Z, Wang J, et al. Folate-targeted pH-sensitive bortezomib conjugates for cancer treatment. *Chem Commun (Camb).* 2019;55(29): 4254-4257

- [31] Tian H, Lin L, Chen J, et al. RGD targeting hyaluronic acid coating system for PEI-PBLG polycation gene carriers. *J Control Release*. 2011;155(1): 47-53.
- [32] Saul JM, Annapragada AV, Bellamkonda RV. A dual-ligand approach for enhancing targeting selectivity of therapeutic nanocarriers. *J Control Release*. 2006;114(3):277-87.
- [33] Kluza E, van der Schaft DW, Hautvast PA, et al. Synergistic targeting of  $\alpha v \beta 3$  integrin and galectin-1 with heteromultivalent paramagnetic liposomes for combined MR imaging and treatment of angiogenesis. *Nano Lett*. 2010; 10(1): 52-8.
- [34] Ying X, Wen H, Lu WL, et al. Dual-targeting daunorubicin liposomes improve the therapeutic efficacy of brain glioma in animals. *J Control Release*. 2010;141(2):183-192
- [35] Noble GT, Stefanick JF, Ashley Jd, et al. Ligand-targeted liposome design: challenges and fundamental considerations. *Trends Biotechnol*. 2014;32(1):32-45.
- [36] Sawant EE, Torchilin Vp. Challenges in Development of Targeted Liposomal Therapeutics. *AAPS J*. 2012;14(2):303-315.
- [36] Tang J, Zhang L, Liu Y, et al. Synergistic targeted delivery of payload into tumor cells by dual-ligand liposomes co-modified with cholesterol anchored transferrin and TAT. In *J Pharm*. 2013;454(1):31-40.

## Figures

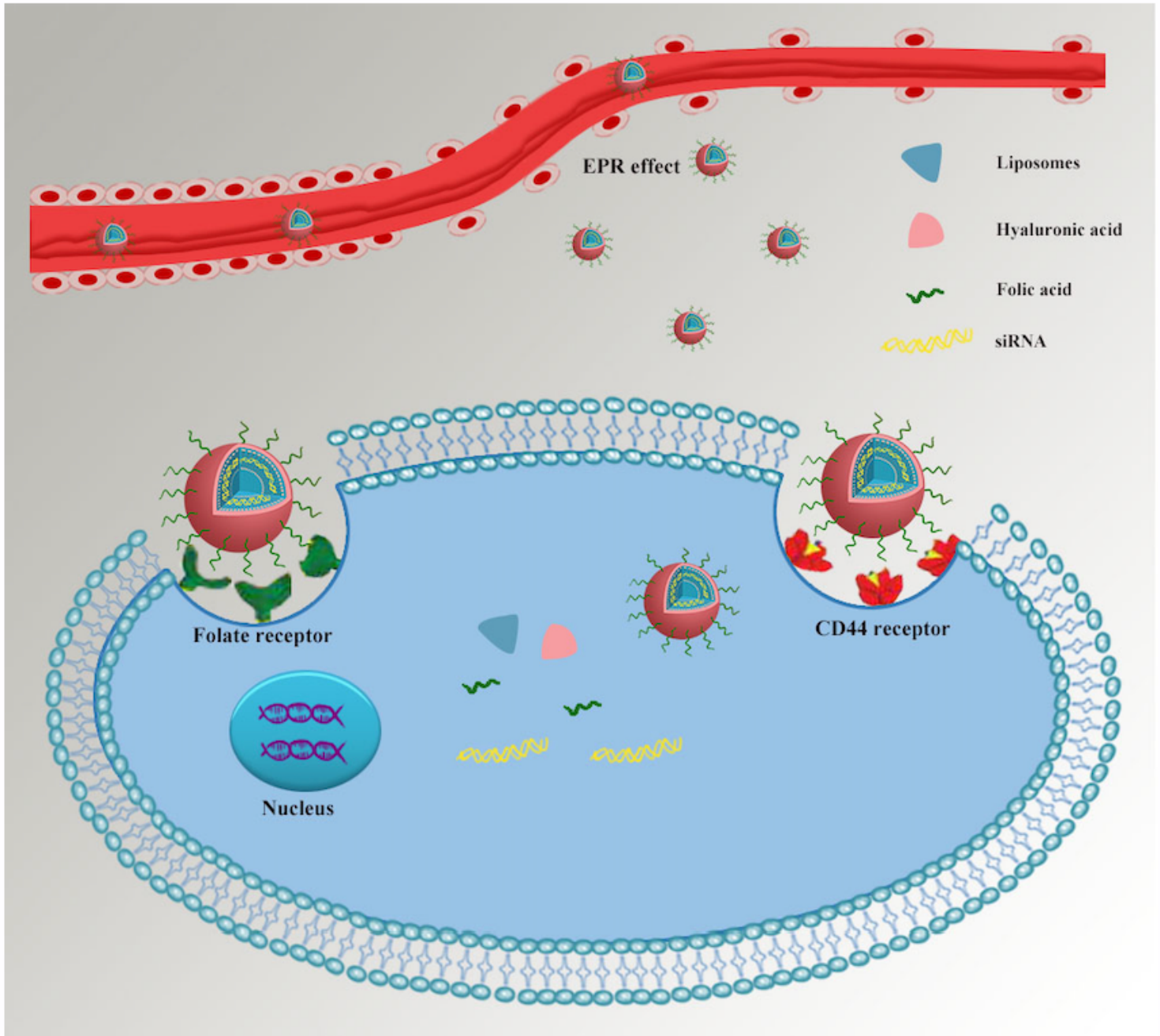


**Figure 1**

The schematic diagram of dual-targeted cationic liposomes (HA-FA-Lip) delivering siBcl-2 to tumor sites

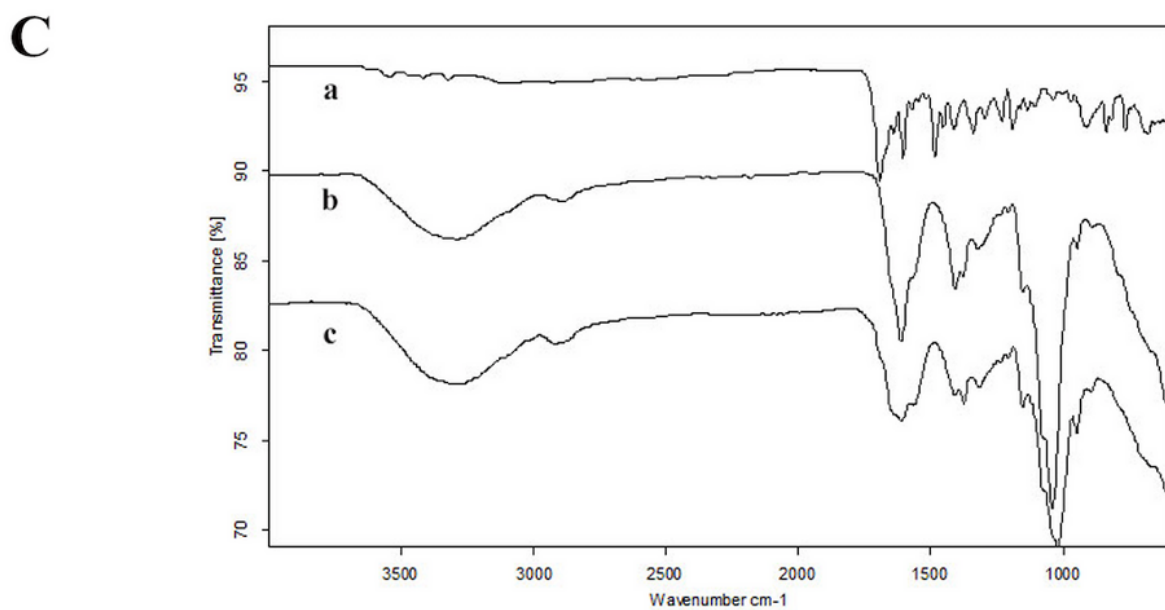
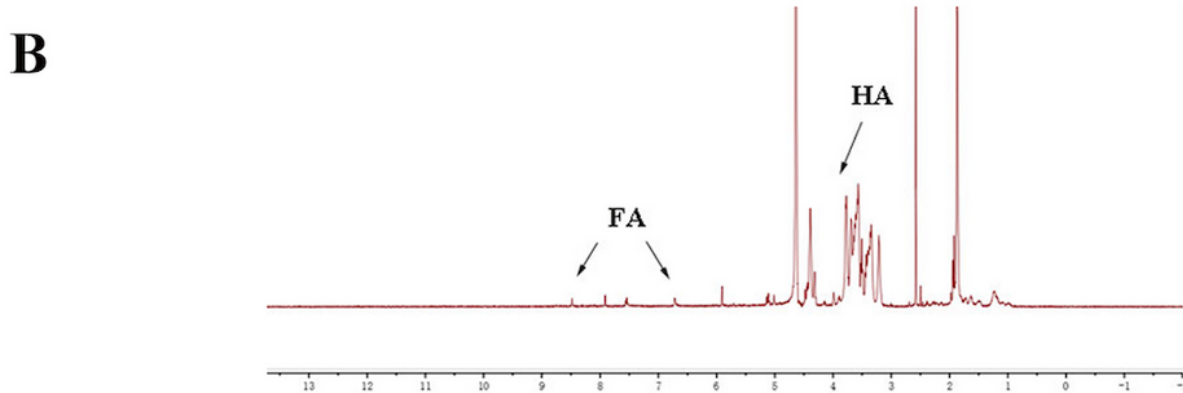
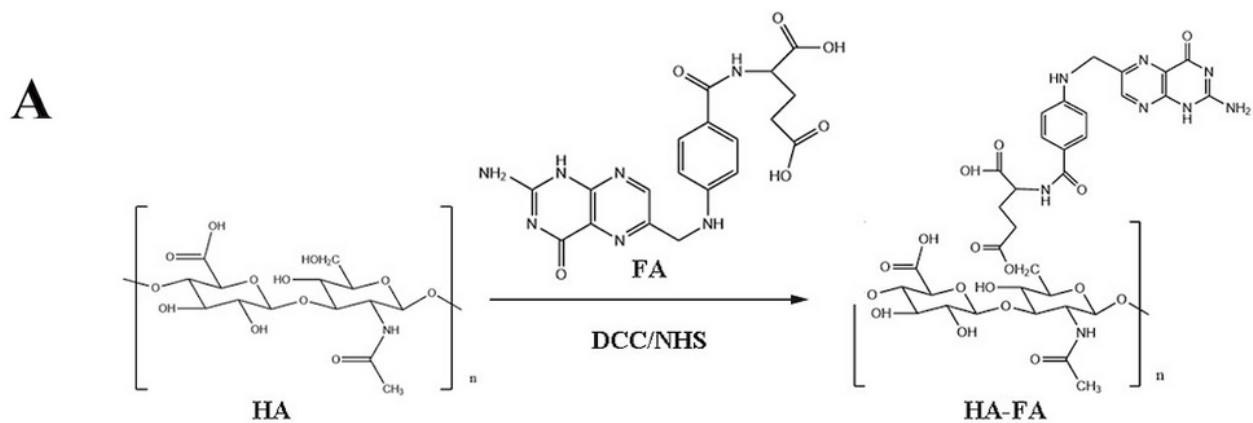


**Figure 2**

(A) Synthesis route of HA-FA; (B)  $^1\text{H}$  NMR spectra of HA-FA polymer; (C) FT-IR spectra of FA, HA and HA-FA.

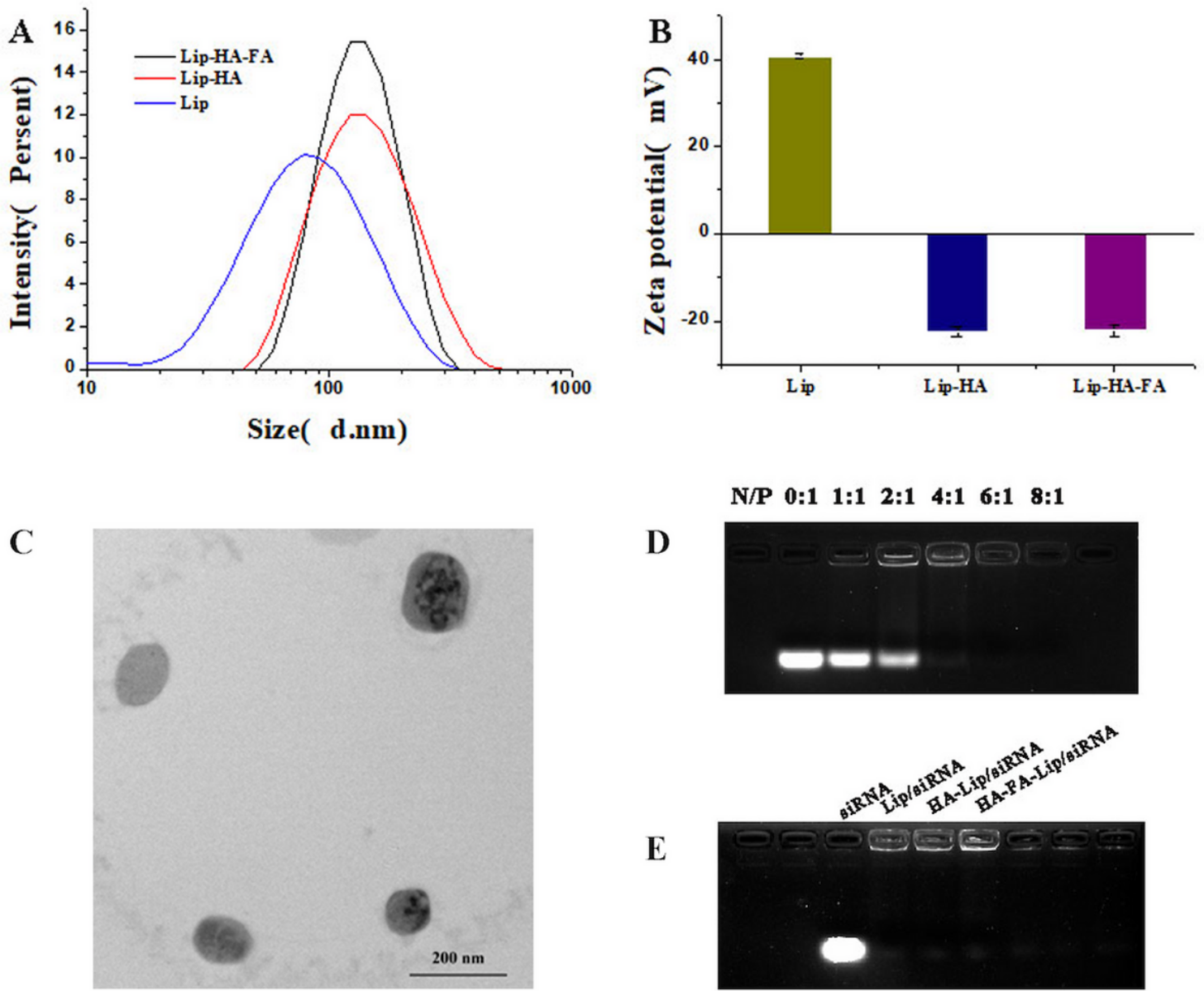


**Figure 3**

Figure 3 shows the characterization of liposomes. (A) Particle size distribution (DLS) of Lip, HA-Lip, and HA-FA-Lip. (B) Zeta potential of Lip, HA-Lip, and HA-FA-Lip. (C) TEM images of HA-FA-Lip. (D) Gel electrophoresis image of Lip/siRNA with different N/P ratio. (E) Gel electrophoresis image of siRNA, Lip/siRNA, HA-Lip/siRNA, and HA-FA-Lip/siRNA at optimal N/P ratio. The results are expressed as the mean  $\pm$  SD (n = 3).

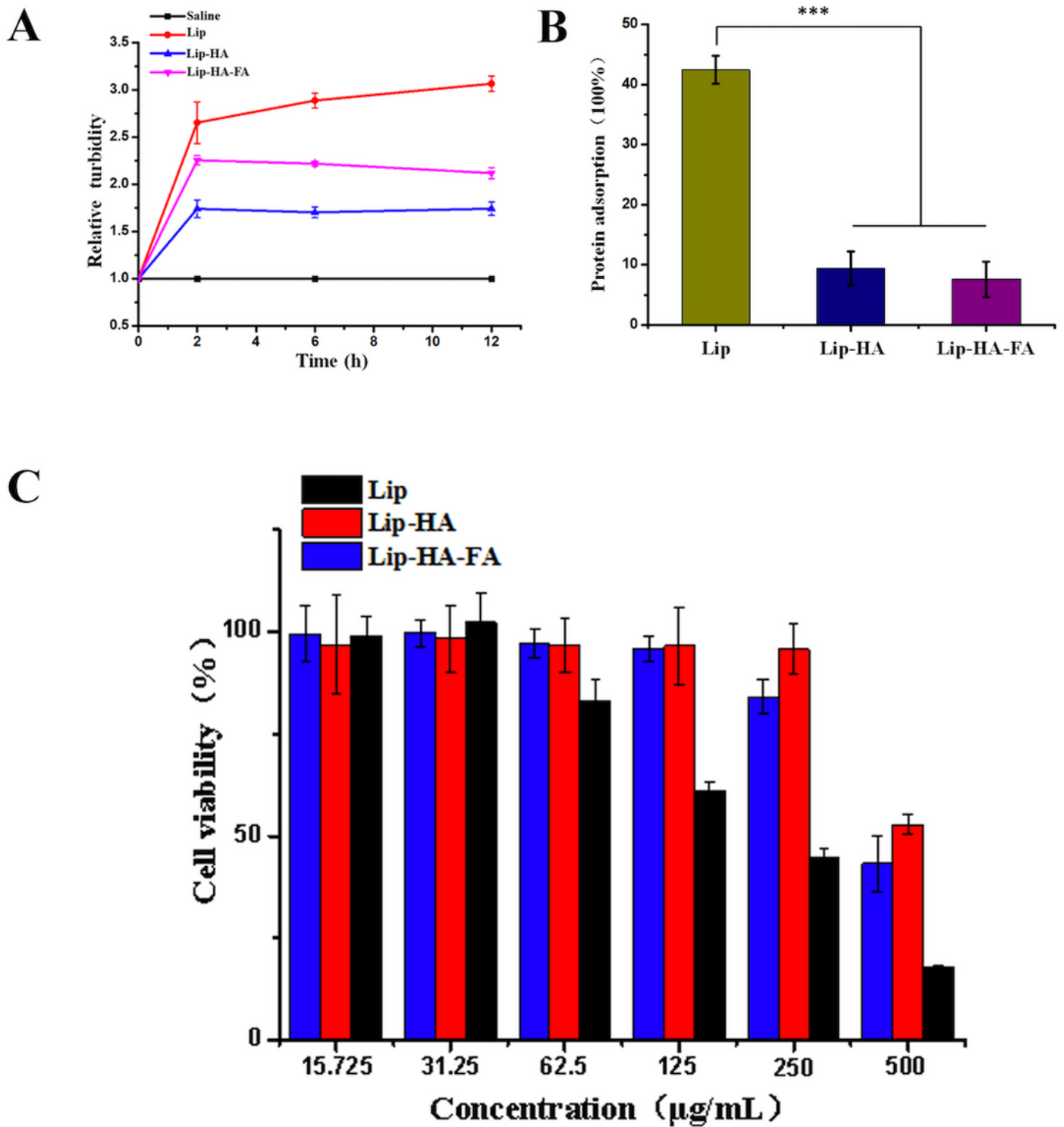
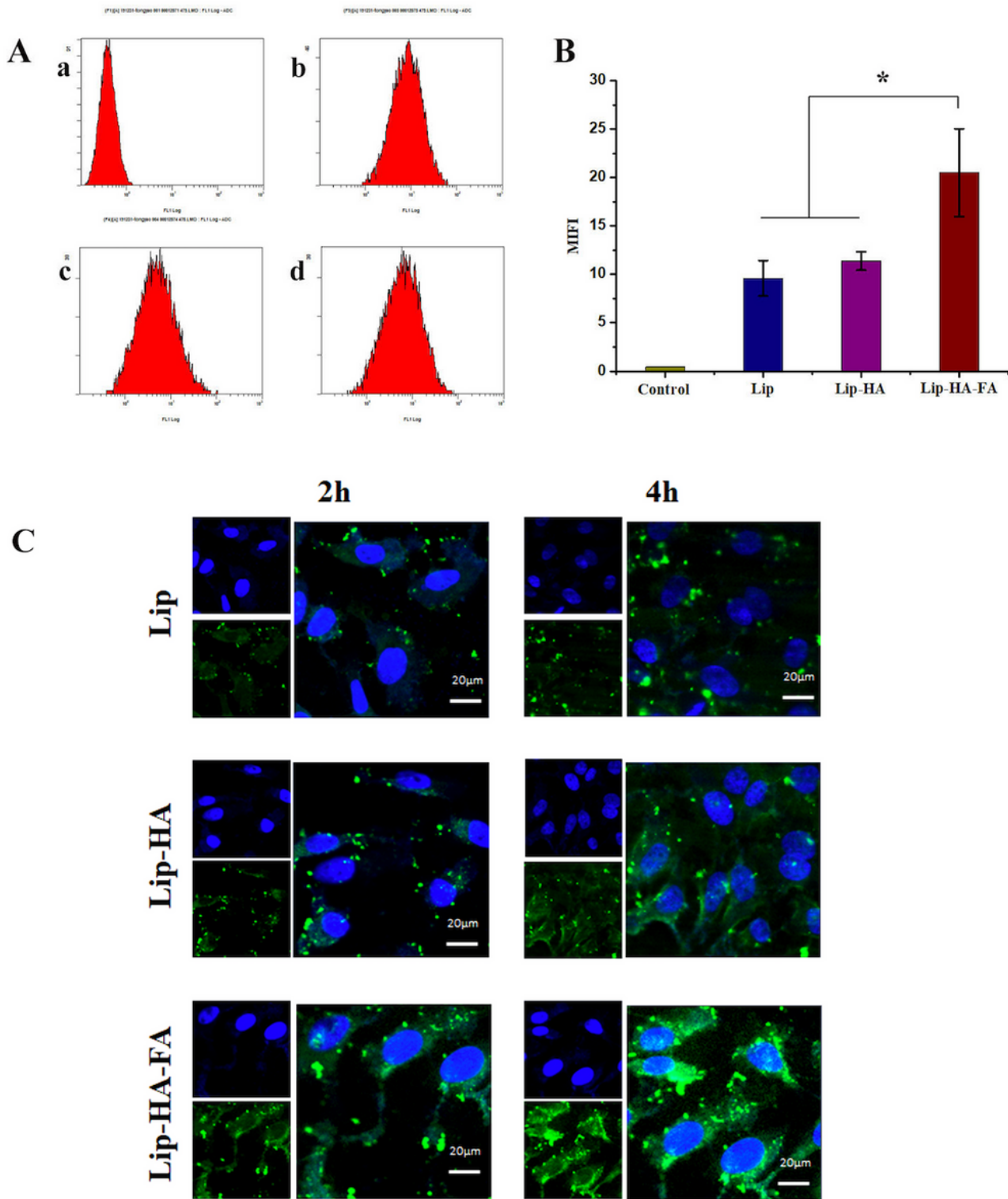


Figure 4

(A) Serum stability and (B) Protein adsorption of Lip, HA-Lip and HA-FA-Lip; (C) Viability of Hela cells after incubation with Lip, HA-Lip and HA-FA-Lip. The results are expressed as the mean  $\pm$  SD (n = 3, \*\*\*p < 0.001)



**Figure 5**

(A) Quantitative uptake of control Control (a) , Lip/siRNA-FAM (b), HA-Lip/siRNA-FAM (c) and HA-FA-Lip/siRNA-FAM (d) by flow cytometry; (B) Mean fluorescence intensity (MFI) of and siRNA-FAM in cell with different treatments ; (C) Cellular distribution of siRNA-FAM in different formulations at 2 h and 4 h by CLSM. The results are expressed as the mean  $\pm$  SD (n = 3, \*p< 0.05)

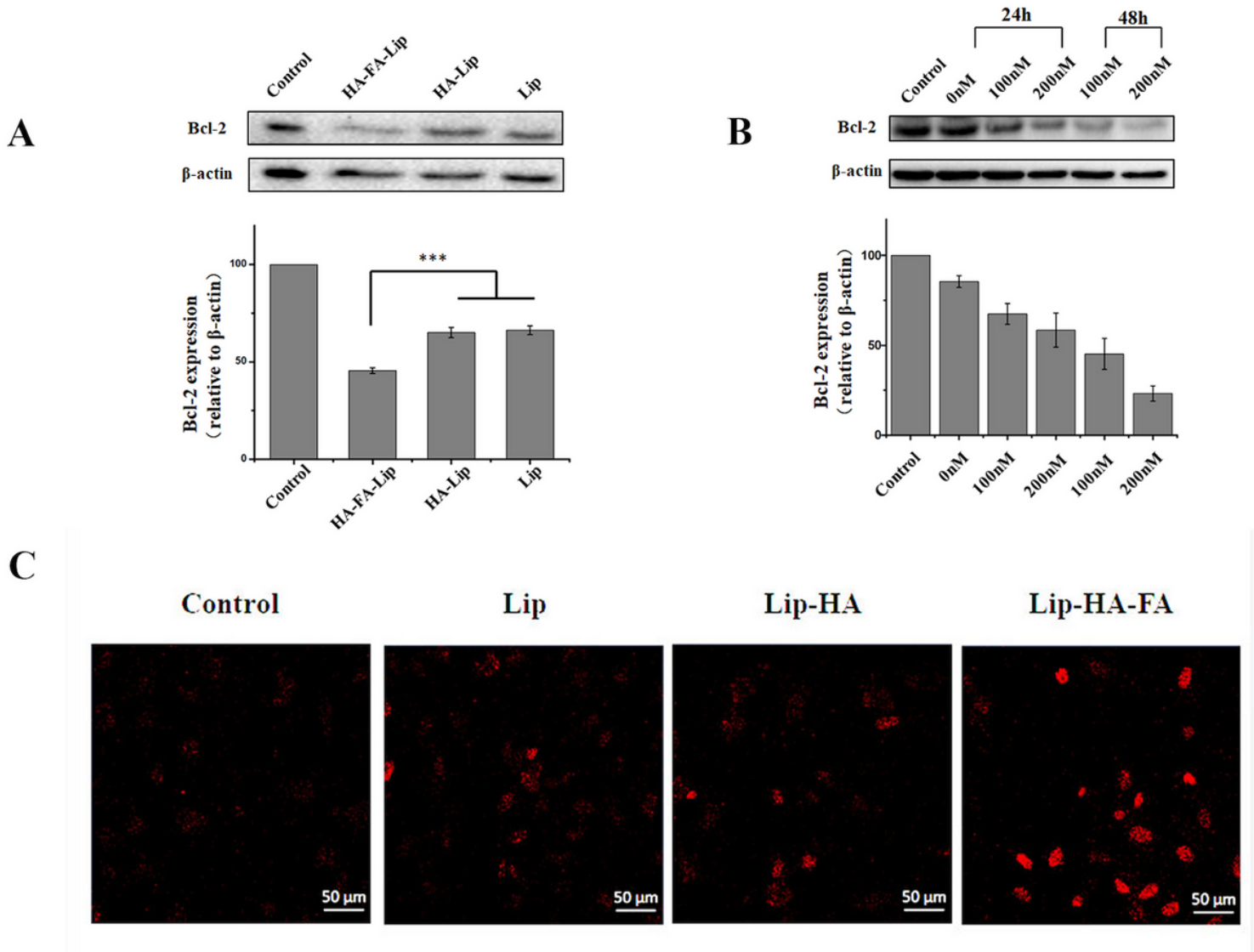


**Figure 6**

(A) Bcl-2 protein expression level of HeLa cells by Western blot after incubation with Lip/siBcl-2, HA-Lip/siBcl-2 and HA-FA-Lip/siBcl-2; (B) In vitro gene silencing effects detected in different transfection conditions ; (C) In vitro cell apoptosis observed by CLSM. The results are expressed as the mean  $\pm$  SD (n = 3,\*\*\*p < 0.001 )

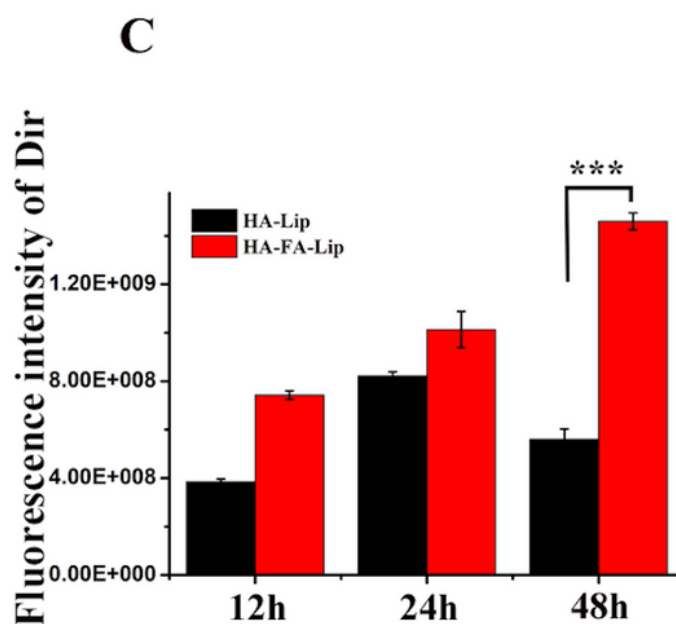
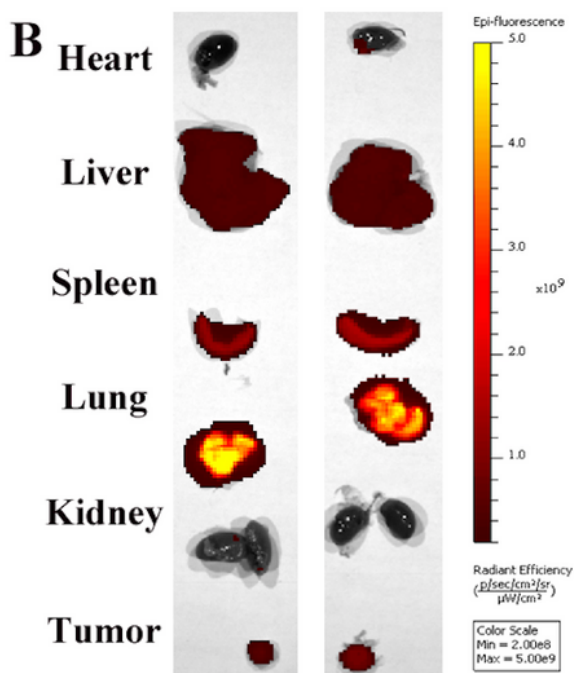
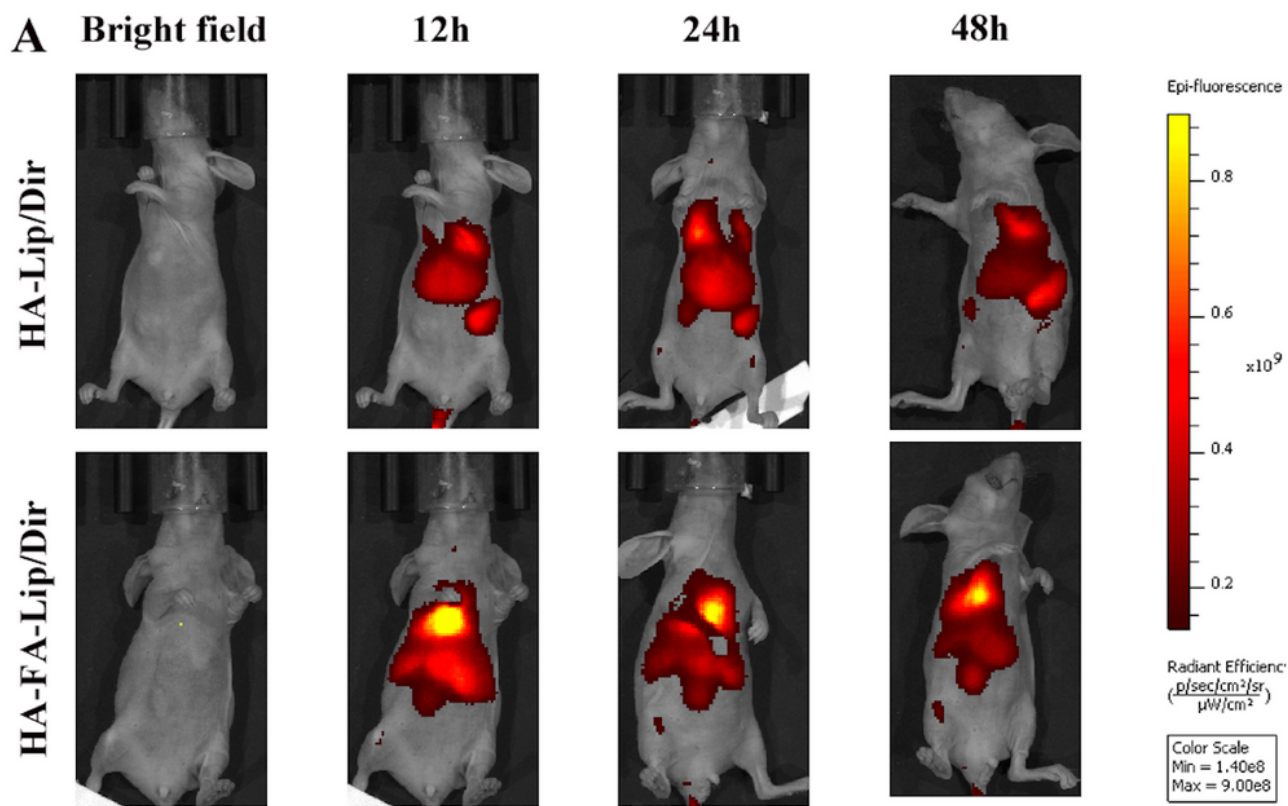


**Figure 7**

(A) HA-Lip/Dir and HA-FA-Lip/Dir distribution obtained by IVIS Spectrum at the certain time; (B) tumors and major organs retrieved to observe fluorescence and distribution after 48h. (C) The Dir fluorescence intensity in tumor. The results are expressed as the mean  $\pm$  SD ( $n=3$ , \*\*\* $p < 0.001$ )

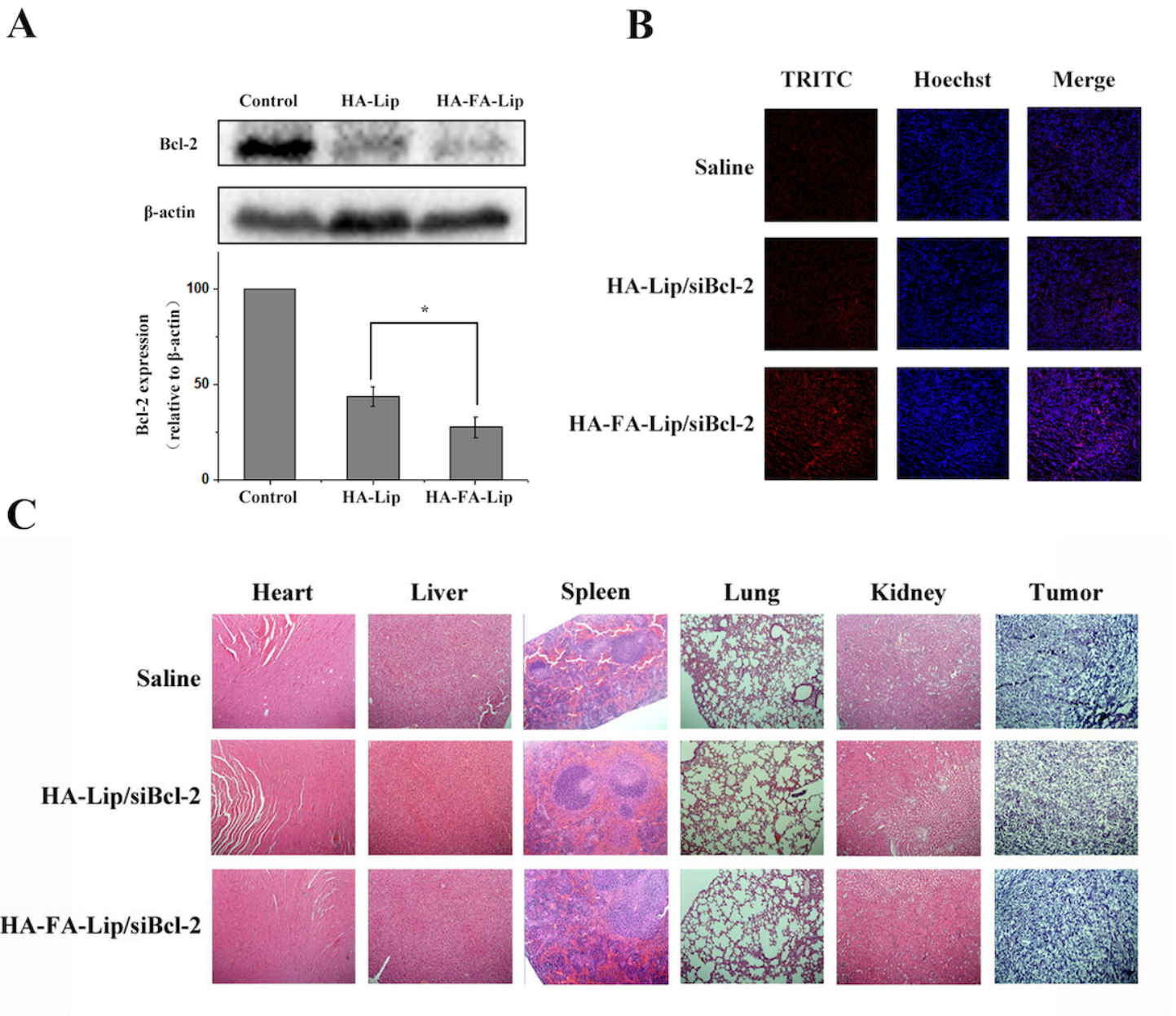


**Figure 8**

(A) The Bcl-2 expression of tumors detected by Western blot; (B) TUNEL staining of tumor harvested from different groups of mice; (C) H&E staining (100 $\times$ ) of heart, liver, spleen, lung, kidney and tumor harvested from different groups of mice. The results were expressed as the mean  $\pm$  SD ( $n=3$ ,  $p<0.05$ ).